

Large Scale Structure as a Probe of Gravitational Slip

Scott F. Daniel*,¹ Robert R. Caldwell,¹ Asantha Cooray,² and Alessandro Melchiorri³

¹*Department of Physics and Astronomy, Dartmouth College, Hanover, NH 03755 USA*

²*Department of Physics and Astronomy, University of California, Irvine, CA 92697 USA*

³*Physics Department and Sezione INFN, University of Rome,
"La Sapienza," P.le Aldo Moro 2, 00185 Rome, Italy*

(Dated: October 22, 2018)

A new time-dependent, scale-independent parameter, ϖ , is employed in a phenomenological model of the deviation from General Relativity in which the Newtonian and longitudinal gravitational potentials slip apart on cosmological scales as dark energy, assumed to be arising from a new theory of gravitation, appears to dominate the universe. A comparison is presented between ϖ and other parameterized post-Friedmannian models in the literature. The effect of ϖ on the cosmic microwave background anisotropy spectrum, the growth of large scale structure, the galaxy weak-lensing correlation function, and cross-correlations of cosmic microwave background anisotropy with galaxy clustering are illustrated. Cosmological models with conventional maximum likelihood parameters are shown to find agreement with a narrow range of gravitational slip.

I. INTRODUCTION

The quest for the source of the cosmic acceleration has lead to speculation that the proper theory of gravitation departs from General Relativity (GR) on cosmological scales. That is, gravitation may be well described using Einstein's theory within the solar system and the environs of the galaxy, but a different theory is required on the scale of the Hubble length (e.g. Ref. [1]). There are numerous examples of a theory capable of producing a late-time acceleration, all of which introduce new gravitational degrees of freedom, with wide-ranging implications for observable phenomena [2, 3]. Given this possible abundance in new physics, it is important to come up with tests that can distinguish between the effects of dark energy and those of modified gravity. Though late-time accelerated cosmic expansion is the principal indicator that a new "dark" physics is needed, it is not the only test such physics must satisfy. A successful cosmology must also agree with measurements related to the growth of perturbations as probed by the cosmic microwave background, clustering of large-scale structure, and weak lensing deflections of light.

The concordance cosmology, Λ CDM within GR, gives very specific predictions for the cosmic expansion and the evolution of inhomogeneities. It has been proposed to evaluate alternative theories of gravitation by testing for violations of these predictions (e.g. Ref. [4]). Efforts along these lines consist of fitting separate Λ CDM parameters to tests of structure growth and cosmic expansion [5], or constraining a phenomenological description of the linear growth rate of density perturbations with galaxy clustering surveys [6, 7, 8, 9]. To within the stated uncertainties, these current results are all consistent with Λ CDM. The absence of any realistic theory of the cosmological constant, however, has prompted many

to question whether gravity itself is the culprit.

An exhaustive study of departures from GR as an explanation for dark energy phenomena is difficult, as Einstein's theory represents a mere island in a sea of possible gravitational theories. Yet, a common feature within a broad range of such theories is a decoupling of the perturbed Newtonian-gauge gravitational potentials ϕ and ψ , defined by the perturbed Robertson-Walker line-element

$$ds^2 = a^2 [-(1 + 2\psi)d\tau^2 + (1 - 2\phi)d\vec{x}^2], \quad (1)$$

using the notation and convention of Ma & Bertschinger [10]. To give a physical sense of these potentials, ψ enters the Newtonian limit of the equation of motion, $\ddot{\vec{x}} = -\vec{\nabla}\psi$, and ϕ enters the Poisson equation $\nabla^2\phi = -4\pi G a^2 \delta\rho$.

Whereas GR predicts $\psi = \phi$ in the presence of non-relativistic matter, a *gravitational slip*, defined as $\psi \neq \phi$, generically occurs in modified gravity theories. This inequality means that the gravitational potential created by a galaxy cluster is not the same potential responsible for the geodesic motion of the constituent galaxies. For primordial cosmological perturbations, the potentials are not completely free, however, as there exists a constraint equation, valid under general assumptions in the long-wavelength limit [11]. Hence, a new relation between these potentials is a launching point for investigations of cosmological manifestations of modified gravitation.

With a view towards testing modified gravitation against large-scale structure, the relation between ϕ and ψ has been examined for scalar-tensor theories [12], generalized gravitational Lagrangians or $f(R)$ theories [13, 14], a tensor-vector-scalar model of gravity [15], the Dvali-Gabadze-Porrati (DGP) model [16, 17, 18], and a Lorentz-invariance violating massive gravity [19]. Phenomenological relations between the potentials have been widely investigated [20, 21, 22, 23, 24, 25, 26]. A general set of post-Friedmannian parameters has also been proposed [27], which reproduces the evolution of ϕ and ψ on both sub- and super-horizon scales for DGP and $f(R)$

*scott.f.daniel@dartmouth.edu

gravities; the relation between these parameters and cosmic acceleration has been discussed in Ref. [28]. Much of the analysis has been formal, with an aim towards future tests. Few efforts have been made to place constraints using current data.

In this paper we explore the parameterized post-Friedmannian (PPF) description of gravitation introduced in Ref. [29] (hereafter CCM). CCM posit a modified theory of gravitation that produces a Λ CDM-equivalent background with perturbations such that $\psi = (1 + \varpi)\phi$, where ϖ is taken to be scale-independent. Here, we correct an important error in CCM, and explore the impact on a wider range of cosmological phenomena. In Sec. II we review the model for the time-dependent quantity ϖ and the description in terms of cosmological parameters. We compare the PPF formalism to similar attempts at modifying GR in the literature. In Sec. III we give the procedure for evolving cosmological perturbations and describe modifications to the CMBfast software [30]. In Sec. IV we explore the influence of ϖ on the cosmic microwave background (CMB) anisotropy, correcting several errors in the numerical calculations described in CCM. We show the effect of $\varpi \neq 0$ on the Wilkinson Microwave Anisotropy Probe (WMAP) [31] best-fit cosmology and its consistency with current data. Using WMAP best-fit cosmological parameters, we similarly demonstrate the effect of $\varpi \neq 0$ on perturbation growth in Sec. V, weak lensing in Sec. VI, and the integrated Sachs-Wolfe effect in Sec. VII. We attempt a synthesis of these results in Sec. VIII, and present a final discussion in Sec. IX.

II. PARAMETERIZATION

Non-Einstein gravitation generically predicts a decoupling of the gravitational potentials, $\phi \neq \psi$, such that the two potentials are independent functions of the four space-time coordinates, τ and \vec{x} :

$$\psi(\tau, \vec{x}) = [1 + \varpi(\tau, \vec{x})] \times \phi(\tau, \vec{x}). \quad (2)$$

The model proposed in CCM attempts to link the departure from GR with the growth of an effective dark energy relative to normal matter and radiation, whereby it was motivated that

$$\begin{aligned} \varpi(\tau, \vec{x}) &= \varpi_0 \rho_{\text{DE}}(\tau, \vec{x}) / \rho_{\text{m}}(\tau, \vec{x}), \\ &\approx \varpi_0 \frac{\bar{\rho}_{\text{DE}}(\tau)}{\bar{\rho}_{\text{m}}(\tau)}. \end{aligned} \quad (3)$$

The second line is obtained by expanding to first order in perturbations on the homogeneous background, indicated by the overbar. Because ϖ already multiplies first order perturbation quantities, the spatial dependence enters at second order and is neglected here. Truly, any theory of gravitational slip must be scale dependent in order to both satisfy solar system constraints at small

length scales and allow for novel cosmological phenomena at extra-galactic length scales. For the purposes of our investigation, focusing on cosmology, ϖ is considered to be homogeneous.

The background evolution is taken to be identical to Λ CDM, in which case

$$\varpi = \varpi_0 \frac{\Omega_{\Lambda}}{\Omega_m} (1 + z)^{-3}. \quad (4)$$

Hence, the gravitational slip remains negligible until late times, when the cosmic acceleration becomes apparent. Our PPF cosmological model is described by the standard set of Λ CDM parameters, plus ϖ_0 . Informally, this model may be referred to as “ $\varpi\Lambda$ CDM”. While there is no *a priori* reason that new gravitational physics should behave this way, this model provides a simple means to test for indications of new gravitational physics. If cosmological data are found to be favoring a non-zero value for ϖ , an advanced theory of gravity beyond GR will be required to explain its value and redshift evolution.

Our parameterization of the relationship between the gravitational potentials can be compared to modifications of GR in the recent literature. Bertschinger & Zukin [26] (hereafter BZ) adopt a notation with $\psi = \Phi_{\text{BZ}}$ and $\phi = \Psi_{\text{BZ}}$ and parameterize

$$\Psi_{\text{BZ}}(\mathbf{k}, t) = \gamma_{\text{BZ}}(a) \Phi_{\text{BZ}}(\mathbf{k}, t) + \dots, \quad (5)$$

with $\gamma_{\text{BZ}}(a) = 1 + \beta a^s$ where β and $s > 0$ are model parameters. In our language (5) takes the form $\phi = \gamma_{\text{BZ}}(a)\psi$, with $\gamma_{\text{BZ}}(a) = 1/(1 + \varpi(a))$ leading to

$$\varpi(a) = -\beta a^s (1 + \beta a^s)^{-1}. \quad (6)$$

In the case $s = 3$ and the limit of small β , the parametrization of BZ agrees with our model (4) for $\beta = -\varpi_0 \Omega_{\Lambda} / \Omega_m$. As we discuss later, CMB anisotropy spectra obtained using the parameterization of equation (6) in our code are fully consistent with the results of BZ. The differences in the CMB anisotropy spectra reported in BZ and CCM are due to a numerical error in the implementation of CCM, which we correct as discussed below.

Hu [28] presents another parameterization with

$$\frac{\Phi_{\text{Hu}} + \Psi_{\text{Hu}}}{2} = g(k, a) \left[\frac{\Phi_{\text{Hu}} - \Psi_{\text{Hu}}}{2} \right] + \dots, \quad (7)$$

with $g(k, a) = g_{\text{SH}}(a) / (1 + c_g^2 k_H^2)$ and $g_{\text{SH}}(a) = g_0 \sqrt{\rho_{\text{de}} \Omega_{\text{tot}} / \rho_{\text{tot}} \Omega_{\text{de}}}$. In our notation the perturbations are now $\phi = -\Phi_{\text{Hu}}$ and $\psi = \Psi_{\text{Hu}}$. Ignoring the momentum dependence, which only dampens the post-Friedmannian modification below a certain scale, the correspondence is found to be

$$\varpi(a) = \frac{-2g(a)}{1 + g(a)}. \quad (8)$$

Given the difference in redshift dependence between equations (4) and (8) for the $g(a)$ used in Ref. [28], a

simple relation between ϖ_0 and g_0 that is accurate at redshifts other than $z = 0$ is not evident. Thus, a detailed comparison is not pursued.

Jain & Zhang [25] present a post-Friedmannian parameterization with $\phi = \eta(k, t)\psi$. Ignoring the momentum dependence, η is related to $\varpi(a)$ through $\varpi(a) = \eta(a)^{-1} - 1$. Since they do not present numerical results on the modification imposed by their parameterization to CMB anisotropies and other large-scale structure observables, a comparison with their work is also not attempted here.

In addition to modifications of gravitation that lead to $\phi \neq \psi$, constraints on possible departures from the Newtonian inverse-square law at cosmological distance scales have also been considered [32, 33]. It is not certain that such modifications satisfy the consistency relation for cosmological perturbations described in Ref. [11]. In any event, our study differs from such works in that no scale-dependent corrections to gravitation are imposed.

III. IMPLEMENTATION OF PPF MODEL

An implementation of the parametrized relationship between the potentials requires a consistent method of treating perturbations in the modified theory. To begin, the phenomenological relation between the gravitational potentials is defined in the conformal-Newtonian (longitudinal) gauge. In practice, however, we find it most convenient to pursue perturbation evolution in the synchronous gauge. Using the notation of Ref. [10], the metric perturbation variables in the two gauges are related as

$$\psi = \frac{1}{2k^2} \left[\ddot{h} + 6\dot{\eta} + \mathcal{H}(\dot{h} + 6\dot{\eta}) \right] \quad (9)$$

$$\phi = \eta - \frac{1}{2k^2} \mathcal{H}(\dot{h} + 6\dot{\eta}), \quad (10)$$

where the dot indicates the derivative with respect to conformal time. In the standard GR case ($\varpi = 0$), the perturbed Einstein equations,

$$k^2\eta - \frac{1}{2}\mathcal{H}\dot{h} = 4\pi Ga^2\delta T_0^0 \quad (11)$$

$$k^2\dot{\eta} = 4\pi Ga^2(\bar{\rho} + \bar{p})\theta \quad (12)$$

$$\ddot{h} + 2\mathcal{H}\dot{h} - 2k^2\eta = -8\pi Ga^2\delta T_i^i, \quad (13)$$

are used to evolve the metric variables, where $(\bar{\rho} + \bar{p})\theta \equiv ik^j\delta T_j^0$ (for greater detail, see [10]). It is standard practice to use the latter two equations (12, 13) for evolution, and apply the first equation (11) as a constraint.

We presume a theory of modified gravitation in which the stress-energy tensor of matter and radiation is conserved, equation (12) remains valid, but equations (11, 13) are invalid. If the perturbed Einstein equations were assumed to remain valid, then the gravitational slip would necessarily imply the existence of new energy density and pressure perturbations which are comoving with

the baryonic and dark matter density perturbations. Furthermore, the non-zero gravitational slip introduces a modification to the perturbed, off-diagonal space-space Einstein equation

$$\dot{\alpha} = -(2 + \varpi)\mathcal{H}\alpha + (1 + \varpi)\eta - 12\pi Ga^2(\bar{\rho} + \bar{p})\sigma/k^2 \quad (14)$$

where $\alpha \equiv (\dot{h} + 6\dot{\eta})/2k^2$. The factor of $1/k^2$ in the last term on the right hand side of (14) corrects a typographical error in CCM equation (8). Note that the shear due to matter and radiation is negligible at late times. This leaves $\dot{\alpha} = -(2 + \varpi)\mathcal{H}\alpha + (1 + \varpi)\eta$ which is simply a restatement of (10) in synchronous gauge. In order to maintain continuity from early times, when GR is valid, to late times, when the gravitational slip becomes significant, equation (14) is used. In turn,

$$\ddot{\alpha} = \dot{\eta}(1 + \varpi) - (2 + \varpi)(\dot{\mathcal{H}}\alpha + \mathcal{H}\dot{\alpha}) + \dot{\varpi}(\eta - \mathcal{H}\alpha) - \frac{d}{d\tau} \left(12\pi Ga^2(\bar{\rho} + \bar{p}) \frac{\sigma}{k^2} \right). \quad (15)$$

Now, instead of evolving equations (12, 13) with constraint (11), equations (12, 14) are evolved with the constraint

$$\dot{h} = 2k^2\alpha - \frac{24\pi Ga^2}{k^2}(\bar{\rho} + \bar{p})\theta \quad (16)$$

derived from α and equation (12). Thus, the time evolution of η , h and α , $\dot{\alpha}$ are fully specified in a modified gravity model.

The above set of equations, corresponding to the recipe R1 of CCM, has been implemented in a modified version of CMBfast [30]. As shown in Appendix A, this prescription satisfies the consistency condition that was first derived in Ref. [11] (equation 2 of BZ). This consistency suggests that our implementation, introduced by CCM, is not fundamentally different from that employed by BZ. Despite the reasons suggested in BZ for differences between the two approaches, consistent results are obtained when the two post-Friedmannian parameterizations are matched.

Note that when presenting results here, the error in the numerical software used by CCM, involving a minus sign error in the $\dot{\varpi}$ term of equation (15), has been corrected. Having rechecked the derivations and software, the revised results for the effect of ϖ on the CMB anisotropy power spectrum are described below.

IV. EFFECTS ON CMB ANISOTROPY

The predicted CMB anisotropy spectra are compared with the WMAP 3-year data, and a likelihood function for the modified gravity variable ϖ_0 is constructed, using the likelihood code supplied by the WMAP team [31]. To avoid duplicating a lengthy search of parameter space, the background cosmology is set to the 3-year WMAP maximum likelihood cosmology (hereafter WMAP3 ML: $\Omega_b = 0.0414$, $\Omega_c = 0.196$, $\Omega_\Lambda = 0.7626$, $h = 0.732$,

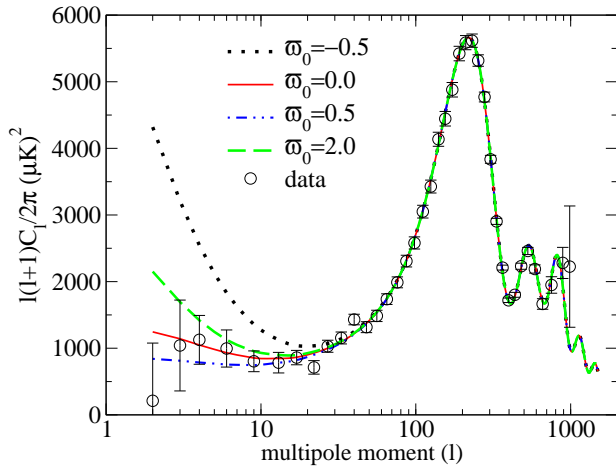


FIG. 1: CMB anisotropy power spectra for different ϖ_0 cosmologies are shown with the binned WMAP 3-year data. All differences are localized to the low multipole moments: the spectra are normalized so that the higher multipole moments for all models are identical to the case of $\varpi_0 = 0$, corresponding to the WMAP3 ML model.

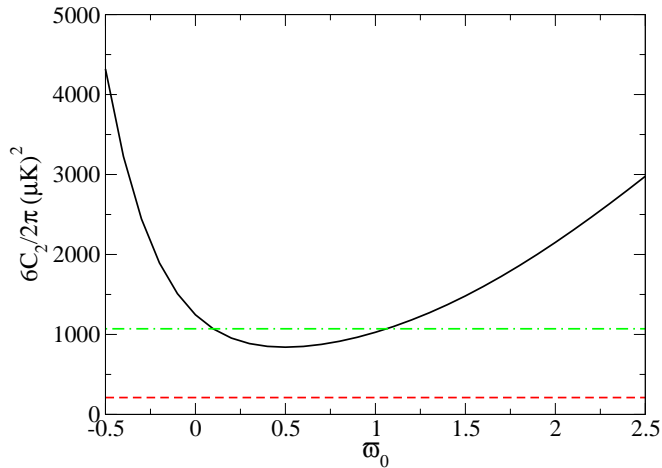


FIG. 2: The predicted CMB temperature anisotropy quadrupole power is shown as a function of ϖ_0 (solid curve). All other parameters are set to the WMAP3 ML cosmology. The central value and 1σ upper bound of the WMAP 3 year data, $6C_2/2\pi = 211 \pm 860$ [31], are shown by the dashed and dot-dashed curves.

$\tau = 0.091$, $n_s = 0.954$), and for comparison to the 3-year WMAP plus SN Gold maximum likelihood cosmology (hereafter WMAP3+SNGold ML: $\Omega_b = 0.0454$, $\Omega_c = 0.2306$, $\Omega_\Lambda = 0.724$, $h = 0.701$, $\tau = 0.079$, $n_s = 0.946$) [34]. Figure 1 plots the multipole moments for several simulations with different values of ϖ_0 in the WMAP3 ML cosmology. Normalizing the spectra to the observed amplitude of the acoustic peaks at $\ell \gtrsim 100$, we see that only the lowest multipole moments, $\ell \lesssim 30$, are affected by ϖ_0 .

Furthermore, we observe that the large-angle anisotropy power grows as $|\varpi_0 - 0.5|$ deviates from

zero. For a closer look, the quadrupole moment is shown as a function of ϖ_0 in Figure 2. This quadratic behavior can be understood as follows. The integrated Sachs-Wolfe effect contribution to the temperature anisotropy depends on $\dot{\phi} + \dot{\psi}$, which varies with ϖ as

$$\dot{\phi} + \dot{\psi} = (3\varpi + (\Gamma - 1)(2 + \varpi)) \mathcal{H}\phi \quad (17)$$

where $\Gamma \equiv 1 + d \ln \phi / d \ln a$. Numerical results show that Γ decreases monotonically, becoming negative with increasing ϖ_0 . Upon squaring the above quantity, it is evident that $|\varpi| \gg 1$ will lead to strong anisotropy in the low multipoles, which are sourced at late times. Note that a similar trend, a local minimum of large-angle anisotropy power as a function of the post-Friedmannian parameter, is seen in Hu's model, in Figure 1 of Ref. [28]. BZ should see the same trend, if a wider range of β is searched than in Figure 5 of Ref. [26].

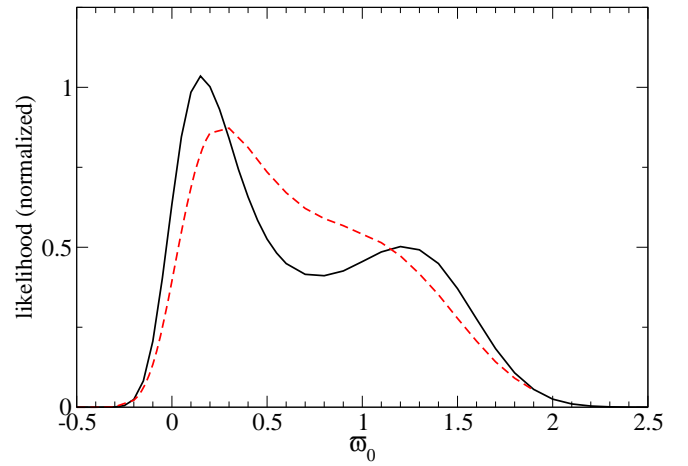


FIG. 3: The likelihood of ϖ_0 due to the CMB, calculated using the November 2006 version of the WMAP likelihood code [31], is shown. All other cosmological parameters are set to the WMAP3 ML (solid curve) or the WMAP3+SNGold ML (dashed curve) model. The results include the TT and TE spectra. The results are consistent with $\varpi_0 = 0$ (Λ CDM), but favor positive values of ϖ_0 . The locations of the primary (left) and secondary (right) likelihood peaks correspond to the range of ϖ_0 for which the predicted quadrupole lies within the 2σ range of WMAP.

The local minimum in the quadrupole amplitude helps explain the double-peaked structure of the WMAP likelihood function, shown in Figure 3. The likelihood is suppressed at large values of $|\varpi_0 - 0.5|$, due to the excessive large angle anisotropy power. And while the low quadrupole moment reported by WMAP has been interpreted to be indicative of new physics, in fact the WMAP likelihood does not necessarily reward an anisotropy spectrum that smoothly leads to low power at low ℓ . The anisotropy spectrum with lowest quadrupole, at $\varpi_0 = 0.5$, is suppressed relative to $\varpi_0 = 0, 1.5$ for the WMAP3 ML parameters, as shown in Figure 3. In the case of the WMAP3+SNGold ML model, which has a slightly higher matter density, the primary peak in the likelihood

distribution is shifted towards a slightly higher value of ϖ_0 . To understand this behavior, note that in the case $\varpi = 0$, the strength of the ISW contribution depends on Ω_m , with $\Gamma \approx (\Omega_m[a])^{0.55}$. An increase in Ω_m thereby diminishes the ISW contribution. Because the WMAP CMB data appears to prefer a moderate ISW contribution, the low quadrupole notwithstanding, then the data should prefer a low matter density at $\varpi_0 = 0$, as seen in Figure 3.

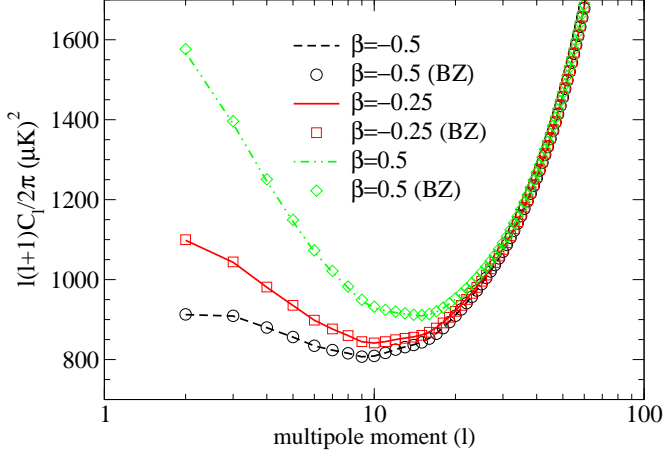


FIG. 4: The equivalence of alternative techniques for evolving cosmological perturbations under PPF gravitation is illustrated by the effect on CMB anisotropy spectra. Lines show the spectra produced following our procedure (equations 14-16) with the parameterization (4) replaced by that proposed in BZ, $\varpi(a) = -\beta a^s / (1 + \beta a^s)$ with $s = 3$. Symbols indicate the spectra produced following BZ's procedure (equations 18-20). The agreement between the techniques is exact.

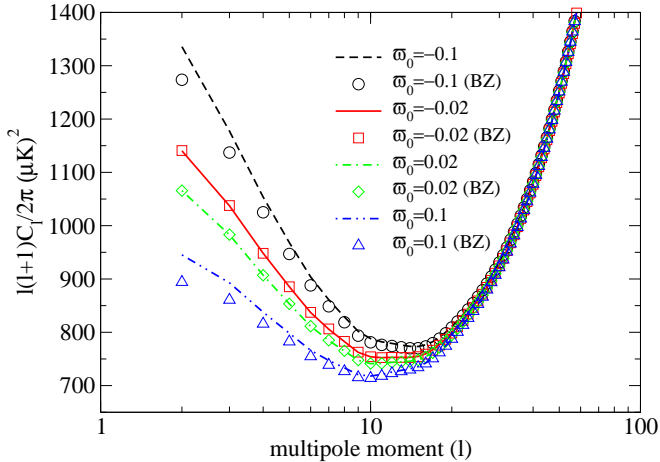


FIG. 5: The effect of the parameterization of gravitational slip on CMB anisotropy spectra is shown. Lines show the spectra produced using our parameterization, equation (4); symbols indicate spectra produced using the BZ's parameterization, $\phi/\psi = 1 + \beta a^s$ with $s = 3$. To compare, the parameter β is set to $\beta = -\varpi_0 \Omega_\Lambda / \Omega_m$. The agreement is excellent in the limit of small β .

Figures 4 and 5 compare the results of BZ with our PPF implementation. To recreate BZ's results, a second CMBfast code was modified to evolve according to GR until $z = 30$. At that point, the parameter

$$\zeta = \frac{2}{3} \frac{\dot{\phi}}{\mathcal{H}} + \phi \quad (18)$$

is calculated, where w is the background equation of state (assuming that only matter and Λ contribute). Next, ζ is set to remain constant for the rest of the calculation, whereupon the evolution is determined by the equations

$$\dot{\phi} = (\zeta - \phi) \left(\mathcal{H} - \frac{\dot{\mathcal{H}}}{\mathcal{H}} \right) - \mathcal{H}\psi \quad (19)$$

$$\dot{\alpha} = \psi - \mathcal{H}\alpha \quad (20)$$

and $\psi = \phi / \gamma_{\text{BZ}}$, $\gamma_{\text{BZ}} = 1 + \beta a^s$, $\eta = \phi + \mathcal{H}\alpha$. Here, (19) comes from equation (2) of BZ and (20) comes from the definition of α . This second code uses none of the Einstein equations. The results, shown in Figures 4 and 5, are equivalent to our results produced using equation (4) if the appropriate relationship between ϖ and γ_{BZ} is imposed. Appendix A demonstrates this equivalence analytically.

V. THE GROWTH OF STRUCTURE

The growth of density perturbations in baryonic and dark matter is affected by gravitational slip, as the potential produced by an overdensity no longer matches the potential responsible for gravitational acceleration. In GR, equations (11) and (13) combine with the fluid conservation law (equation 29a in Ref. [10]),

$$\dot{\delta} = -(1+w) \left(\theta + \frac{\dot{h}}{2} \right) - 3\mathcal{H} \left(\frac{\delta p}{\delta \rho} - w \right) \delta, \quad (21)$$

to give the equation for the growth of non-relativistic, pressureless perturbations:

$$\ddot{\delta} + \mathcal{H}\dot{\delta} = 4\pi G a^2 \delta \rho. \quad (22)$$

In the case $\varpi \neq 0$, an *independent* differential equation for the matter density contrast is not readily available as equations (11,13) have been eliminated. CCM try to circumvent this obstacle, using (12,14) and α , together with the assumption of negligible shear to arrive at

$$\ddot{\delta} + \mathcal{H}\dot{\delta} = k^2(1+\varpi)(\mathcal{H}\alpha - \eta). \quad (23)$$

Unfortunately, that is as far as CCM can go without postulating another perturbed fluid $\delta\rho_{\text{DE}}$ to account for the theory's departure from (11). However, there is no barrier to evolving δ – it is simply obtained numerically from (21).

The modified Boltzmann code CMBfast calculates δ as a function of time in the process of calculating the

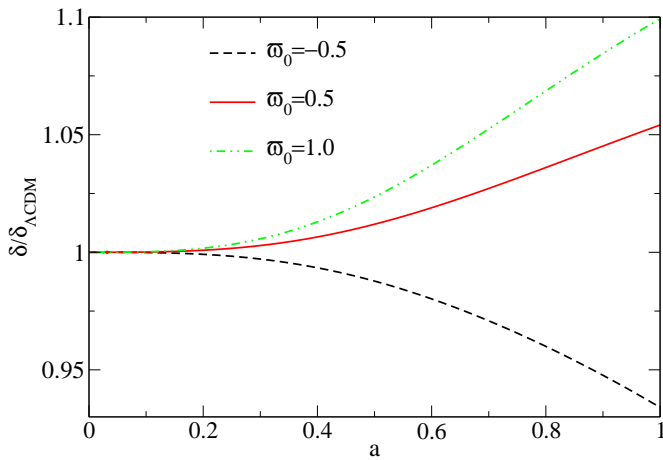


FIG. 6: The matter density contrast as a function of scale factor is shown for different values of ϖ_0 . The density contrast is normalized to a $\varpi_0 = 0$ model. All models use WMAP3 ML parameters.

anisotropy spectrum. Figure 6 illustrates the effect of $\varpi_0 \neq 0$ on the growth of long wavelength matter density perturbations. This effect is monotonic with $\varpi_0 > 0$ enhancing the growth at late times and $\varpi_0 < 0$ suppressing it. By comparing the rate of growth for models with different values of ϖ_0 and Ω_m , an approximate mapping for the growth of δ from $\varpi\Lambda$ CDM to Λ CDM models has been obtained. Specifically, to a good approximation, the growth of structure in a $\varpi_0 \neq 0$ cosmology is equivalent to a Λ CDM cosmology with

$$\Omega_m|_{\Lambda\text{CDM}} = \Omega_m|_{\varpi\Lambda\text{CDM}} + 0.13\varpi_0 \quad (24)$$

In the parameter ranges $-0.5 \leq \varpi_0 \leq 0.5$ and $0.2 \leq \Omega_m|_{\varpi\Lambda\text{CDM}} \leq 0.5$, this fit is good to the 3% level for $a \geq 0.2$. (See Figure 7). Note that $\varpi_0 \neq 0$ does not change the shape of the (linear) matter power spectrum.

Figure 8 plots the predicted dimensionless linear growth rate, $f = d \ln \delta / d \ln a$, against a compilation of recent data. In the future, this may provide an alternative test of modified gravitation. Unfortunately, the current uncertainties in f are too large to provide a meaningful constraint on ϖ_0 .

VI. WEAK LENSING

Gravitational lensing phenomena depends directly on the sum of the two gravitational potentials, and is therefore an excellent probe of gravitational slip. In the cosmological setting, measurements of weak lensing of the pattern of galaxy clustering can be used to constrain ϖ_0 . Proceeding, the E-mode weak lensing convergence correlation function, ξ_E [36], is calculated, which requires the

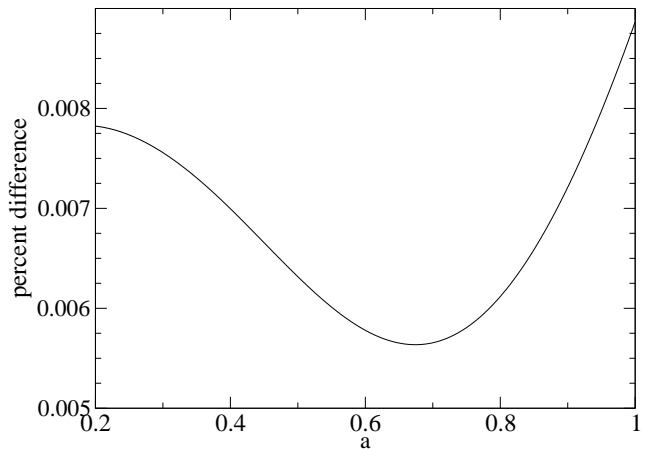


FIG. 7: The goodness of fit of the mapping of the growth rate between $\varpi\Lambda$ CDM and Λ CDM models, is illustrated. The percent difference in the density contrast for a model with $\varpi_0 = 0.4$, $\Omega_m = 0.3$, and a Λ CDM model with $\Omega_m = 0.35$. These cosmologies are predicted to be equivalent by equation (24).

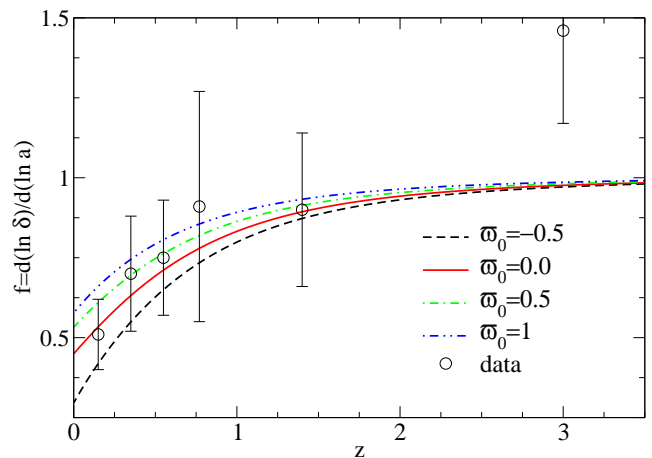


FIG. 8: The dimensionless linear growth rate f plotted as a function of z for different ϖ_0 cosmologies with the WMAP3 ML background. The data point at $z = 0.77$ is due to Ref. [35]. The remaining, hybrid set of data points are taken from Table 1 of Ref. [9], and are based on estimates of large-scale structure power spectrum growth at different redshifts.

convergence power spectrum, given by [37, 38, 39, 40]

$$P_\kappa(l) = l^4 \int_0^{\chi_h} d\chi \frac{n^2(\chi)}{r^4(\chi)} P_{\phi+\psi}^{\text{nonlin}} \left(k = \frac{l}{r(\chi)}, \chi \right) \quad (25)$$

$$n(\chi) = \int_\chi^{\chi_h} d\chi' p(\chi') \frac{r(\chi' - \chi)}{r(\chi')} \quad (26)$$

where χ is the comoving radial distance with χ_h is the horizon distance, $r(\chi)$ is the comoving angular distance (χ in the case of a flat universe), $p(\chi)$ is the probability distribution of lensed sources, and 0 refers to the present epoch.

The lensing convergence depends on the power spec-

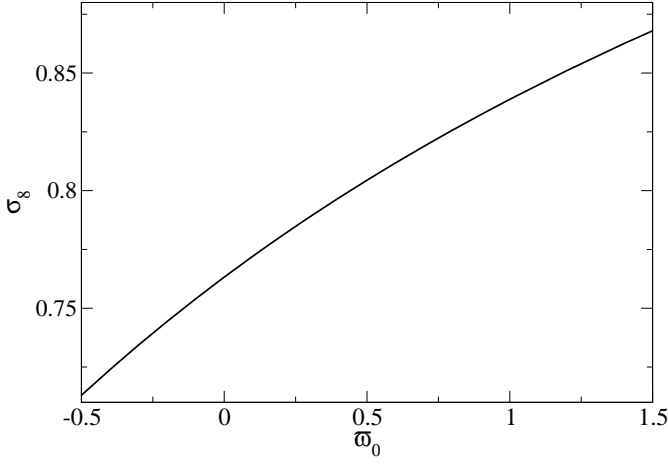


FIG. 9: The values of σ_8 resulting from the normalization to the WMAP 3-year anisotropy power spectrum, are shown as a function of ϖ_0 . All other cosmological parameters are set to match the WMAP3 ML model.

trum of metric perturbations $\phi + \psi$. At linear scales, the power spectrum can be expressed through the power spectrum of density perturbations δ by making use of the growth function $D_\varpi = \delta(z)/\delta(z=0)$ to account for the redshift growth of perturbations and the Poisson equation. Using the relation between ϕ and ψ , we can write

$$P_{\phi+\psi}(k, z) = \frac{9}{4} \Omega_{m,0}^2 \left(\frac{H_0}{ck} \right)^4 \left(\frac{D_\varpi(z)}{a(z)} \right)^2 \left[\frac{2 + \varpi(z)}{2} \right]^2 \times P_{\delta\delta}(k, z = 0), \quad (27)$$

where $P_{\delta\delta}$ is the power spectrum of density perturbations today. Because the length scales probed by the weak lensing measurements extend into the non-linear regime, this description must be extended in order to compute the non-linear matter power spectrum. Since we do not have a complete description of non-linear evolution under modified gravity, here we employ the same technique as used for the usual GR predictions of lensing statistics. We use the fitting function from Peacock and Dodds [41] (PD) to get $P_{\delta\delta}^{\text{nonlin}}$ from the linear power spectrum calculated with our modified CMBfast code. Note that PD's factor $g_{PD}(\Omega, a) = \delta(a)/a$ is meant to compare the growth history to that of an $\Omega_m = 1$ model [42], so $\delta(a)$ normalized at an early redshift is used. Specifically the density contrast is set to $\delta(a = 0.01) = 0.01$ for all ϖ_0 models. The linear power spectrum amplitude is set by the normalization of the CMB anisotropy spectrum to the WMAP 3 year data. In Figure 9 we highlight the relation between σ_8 as a function of ϖ_0 and note that an increase in ϖ_0 has a similar effect of enhancing weak lensing as does an increase in σ_8 in standard Λ CDM cosmologies. For $\varpi_0 = 0$, the GR case, we recover the WMAP3 ML preferred value of $\sigma_8 = 0.76$ [34].

From the convergence spectrum, we can then find the

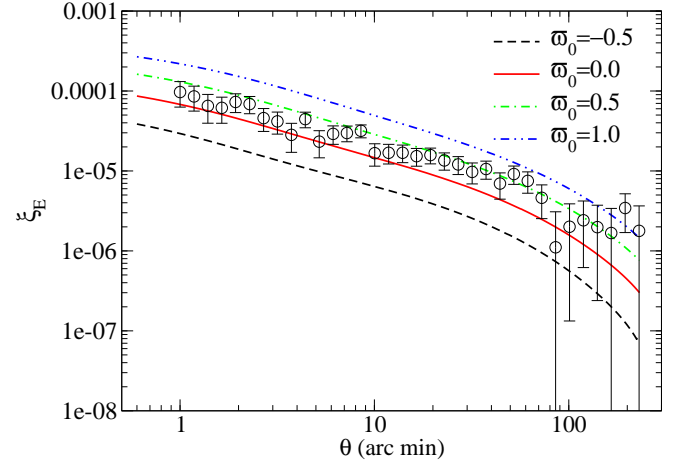


FIG. 10: Model predictions of ξ_E for different values of ϖ_0 . Data is taken from Table B.1 of [43]. The background cosmology is the WMAP3 ML. The power spectrum amplitude is determined by the normalization to WMAP.

modes of the correlation function [44, 45, 46, 47]

$$\begin{aligned} \xi_+(\theta) &= \frac{1}{2\pi} \int_0^\infty dk k P_\kappa(k) J_0(k\theta) \\ \xi_-(\theta) &= \frac{1}{2\pi} \int_0^\infty dk k P_\kappa(k) J_4(k\theta) \\ \xi'_-(\theta) &= \xi_-(\theta) + 4 \int_0^\infty \frac{d\theta'}{\theta'} \xi'_-(\theta') - 12\theta^2 \int_0^\infty \frac{d\theta'}{\theta'^3} \xi_-(\theta') \\ \xi_E(\theta) &= \frac{\xi_+(\theta) + \xi'_-(\theta)}{2} \end{aligned} \quad (28)$$

where $J_i(l)$ are Bessel functions of the first kind. Figure 10 plots $\xi_E(\theta)$ for different ϖ models with the WMAP3 ML cosmology. Varying ϖ_0 results in a multiplicative shift in ξ_E .

Figure 11 plots the likelihood derived from the weak lensing shear correlation function as measured by the Canada-France-Hawaii Telescope Legacy Survey [48] and presented in Table B.1 of Fu *et al.* [43]. The source distribution $p(\chi)$ is taken from equation (14) and Table 1 of Ref. [43]. Unlike the CMB anisotropy spectra, the weak lensing shear correlations functions do not “bounce” with ϖ_0 , so the resulting likelihood function, shown in Figure 11, is narrower and peaks at $\varpi_0 \approx 0.3$. This result excludes $\varpi_0 = 0$, but is roughly consistent with the primary peak in the CMB likelihood, shown in Figure 3.

The exclusion of $\varpi_0 = 0$ based on CMB and weak lensing data in the WMAP3 ML model is not significant at this stage. Only a single parameter in a multi-dimensional parameter space has been searched. Indeed, a positive value of ϖ_0 is expected since we have normalized the underlying density power spectrum to the WMAP3 preferred value of σ_8 , whereas analyses of the weak lensing data have found a preferred normalization value with $\sigma_8 \sim 0.8$, which is slightly higher than the CMB value. The disagreement between these two values is now resolved by a non-zero value for ϖ_0 . While

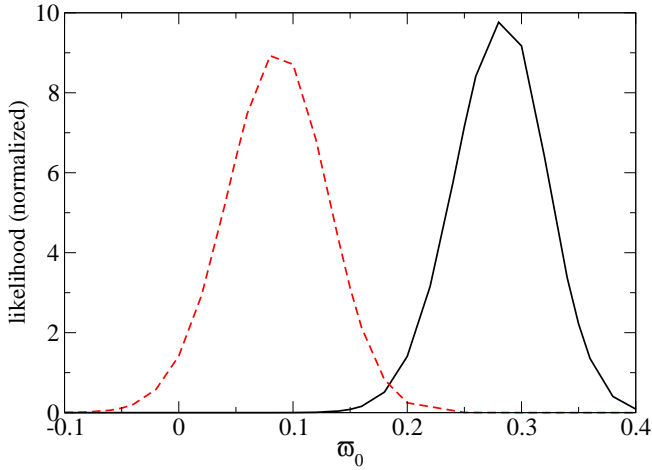


FIG. 11: The likelihood of different ϖ_0 models according to the ξ_E data collected by the Canada-France-Hawaii Telescope Legacy Survey and presented in Table B.1 of Ref. [43] is shown with parameters set by the WMAP3 ML model (solid line) as well as the WMAP3+SNGold ML model (dashed line).

such a difference between CMB and low-redshift matter perturbations is generally the very type of behavior we should look for in modified gravitation scenarios, the fact that we do not perform a joint combined analysis of CMB and weak lensing data precludes us from making a strong statement.

We expect a degeneracy in the effect of ϖ_0 and $\Omega_m h^2$ on the weak lensing predictions, as both parameters control the growth rate of fluctuations. Specifically, increasing ϖ_0 enhances fluctuation growth, as seen in Figure 6, just as does increasing the abundance of clustering matter. By raising $\Omega_m h^2$ the likelihood is expected to peak at lower values of ϖ_0 . This is precisely illustrated in Figure 11, wherein the weak lensing likelihood for ϖ_0 is shown for cosmological models with parameters set by the WMAP3+SNGold ML model, which has a slightly higher matter density. This new likelihood is indeed consistent with lower values of ϖ_0 , including zero.

VII. CMB AND LSS CROSS-CORRELATIONS

A deviation from GR leaves an imprint on the cross-correlation between the CMB and large-scale structure. In order to identify such a signal, we define the two-point angular cross-correlation between the temperature ISW anisotropy and the dark matter fluctuation as [49, 50, 51, 52]

$$C^X(\theta) = \langle \Delta_{ISW}(\hat{\gamma}_1) \delta_{LSS}(\hat{\gamma}_2) \rangle, \quad (29)$$

where the angular brackets denote the average over the ensemble and $\theta = |\hat{\gamma}_1 - \hat{\gamma}_2|$. For computational purposes it is convenient to decompose $C^X(\theta)$ into a Legendre se-

ries such that,

$$C^X(\theta) = \sum_{l=2}^{\infty} \frac{2l+1}{4\pi} C_l^X P_l(\cos(\theta)), \quad (30)$$

where $P_l(\cos \theta)$ are the Legendre polynomials and C_l^X is the cross-correlation power spectrum given by [50, 51, 53, 54]

$$C_l^X = 4\pi \frac{9}{25} \int \frac{dk}{k} \Delta_{\mathcal{R}}^2 I_l^{ISW}(k) I_l^{LSS}(k), \quad (31)$$

where $\Delta_{\mathcal{R}}^2$ is the primordial power spectrum. The integrand functions $I_l^{ISW}(k)$ and $I_l^{LSS}(k)$ are defined respectively as

$$I_l^{ISW}(k) = - \int e^{-\kappa(z)} \frac{d((2+\varpi)\phi_k)}{dz} j_l[kr(z)] dz \quad (32)$$

$$I_l^{LSS}(k) = b \int \Phi(z) \delta^k(z) j_l[kr(z)] dz, \quad (33)$$

where ϕ_k and δ^k are the Fourier components of the gravitational potential and matter perturbation, respectively; Φ is the galaxy survey selection function; $j_l[kr(z)]$ are the spherical Bessel functions; $r(z)$ is the comoving distance at redshift z and $\kappa(\tau) = \int_{\tau}^{\tau_0} \dot{\kappa}(\tau) d\tau$ is the total optical depth at time τ .

A change in ϖ could therefore change not only the value of I_l^{ISW} but also its sign with respect to I_l^{LSS} . Direct measurements of the cross-power spectrum C_l^X are more robust for likelihood parameter estimation since these data would be less correlated than measurements of $C^X(\theta)$. Therefore, the cross-power spectrum C_l^X is computed for different values of ϖ_0 assuming a galaxy survey with a selection function as

$$\Phi(z) \sim z^2 \exp[-(z/\bar{z})^{1.5}] \quad (34)$$

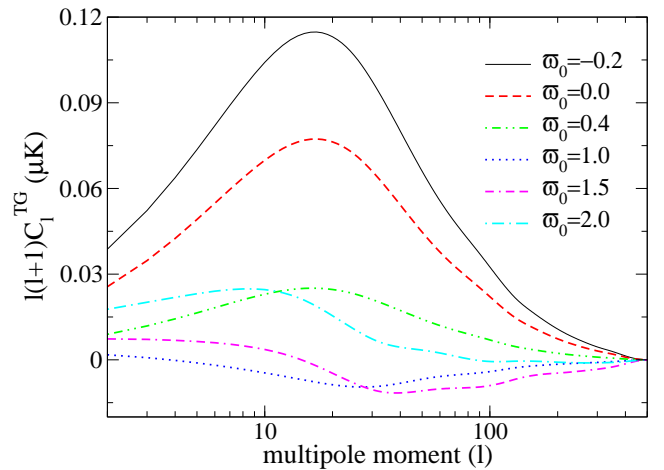


FIG. 12: The cross-correlation angular power spectrum between CMB temperature (ISW) and galaxy distribution is shown as a function of ϖ_0 . A value of $0.5 < \varpi_0 < 1.5$ changes the sign of the ISW, resulting in a negative cross-correlation, in conflict with observations.

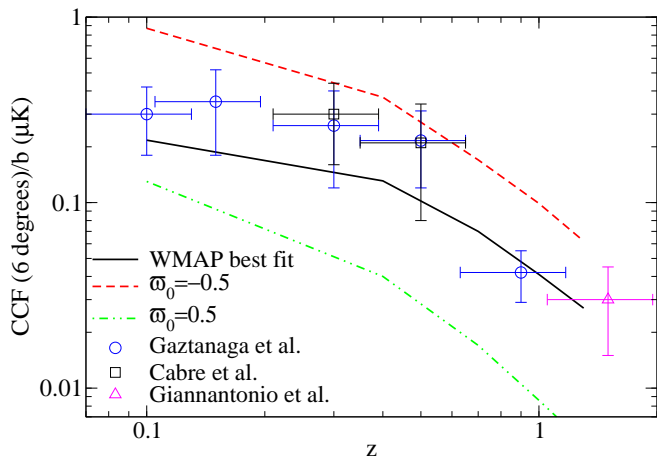


FIG. 13: The cross-correlation amplitude at $\theta = 6$ degrees is shown as a function of redshift for different samples of LSS and WMAP data. The curves show the expected correlation with ϖ_0 varied. The data plotted here comes from the compilation in Ref. [60], making also use of data from Gaztanaga *et al.* [61] (circles), Cabre *et al.* [62] (squares), and Giannantonio *et al.* [60] (triangle).

where \bar{z} , the median redshift of the survey, is $\bar{z} = 0.25$. In recent years, the WMAP temperature anisotropy maps have been cross-correlated with several surveys of Large Scale Structure (LSS) distributions and a positive correlation signal has been detected [55, 56, 57, 58, 59, 60]. As seen in Figure 12, values of $\varpi_0 > 0.5$ would result in anti-correlation and a negative angular spectrum, in disagreement with current observations at the $\sim 2\sigma$ level.

In order to obtain a more quantitative result, the ISW-Galaxy theoretical correlation function for different values of ϖ is compared with the current data as reported in Ref. [60] under the assumption of the WMAP ML model.

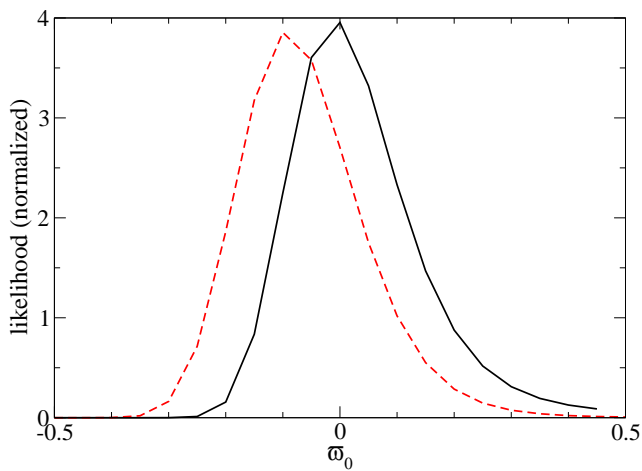


FIG. 14: The likelihood of different ϖ_0 models using current ISW-galaxy cross correlation data is shown. All other cosmological parameters are fixed to the WMAP3 ML model (solid line) or the WMAP3+SNGold ML model (dashed line).

The data and some model curves under modified gravity are shown in Figure 13. The likelihood is reported in Figure 14, consistent with no indications for modified gravity. This constraint should be considered with caution, since the full parameter space has not been explored and the ISW signal may certainly be highly sensitive to changes in parameters such as the matter density and the Hubble constant.

Qualitatively, the ISW-Galaxy theoretical correlation may be understood by considering the path of a CMB photon through a region on the sky containing an abundance of galaxies. As the photon passes through the collective gravitational potential of the clustered galaxies, the decay of the gravitational potential in a Λ CDM cosmology with $\varpi_0 = 0$ leads to the blueshifting of the photon. A negative value of ϖ_0 suppresses the clustering and causes the photon to be further blueshifted as it climbs out of the weakening gravitational potential. The coincidence of the hot spot in the CMB resulting from the blueshifted photons, with the abundance of galaxies on the sky explains a positive cross-correlation. Likewise, a large ϖ_0 enhances clustering and reduces the blueshifting as the photon climbs out of the growing gravitational potential. In extreme cases, the enhanced clustering causes the photon to be redshifted, thereby leading to a negative cross-correlation. The degeneracy between ϖ_0 and $\Omega_m h^2$ suggests that a preference for $\varpi_0 < 0$ seen in Figure 14, will be enhanced by increasing $\Omega_m h^2$: the slower decay of the gravitational potential ($\Gamma \rightarrow 1$ in equation 17) due to the increased matter density is compensated by the reduced clustering with larger ϖ_0 . Figure 14 also shows the fit to current ISW-galaxy cross correlation data using the WMAP3+SNGold ML model parameters, for which the matter density is slightly higher than the WMAP3 ML model. Indeed, the peak of the likelihood shifts to even more negative values, as expected.

VIII. SYNTHESIS

We have examined the consequences of the proposed PPF model of gravitational slip for predictions of the cosmic microwave background anisotropy, the growth of large scale structure, weak lensing, and the ISW-galaxy cross-correlation. The likelihood distributions in ϖ_0 using the WMAP3 ML model parameters are summarized in Figures 15, and using the WMAP3+SNGold ML model parameters in Figure 16. The weak lensing is clearly the most sensitive to ϖ_0 , followed by the ISW-galaxy cross-correlation, and then the CMB.

In the case of the WMAP3 ML model parameters, shown in Figure 15, the overlap between the three distribution functions is strongest near $\varpi_0 \approx 0.2$. However, there is no concordance due to the tension between the values $\varpi_0 > 0$ indicated by the CMB and weak lensing data, and the values centered on zero for the ISW-galaxy cross-correlation. This tension appears to be related to the disagreement in the best-fit σ_8 values derived from

measurements of the CMB and large scale structure. In fact, the additional degree of freedom introduced by ϖ_0 seems to be justified by the sharp peak in the weak lensing distribution.

To find concordance among the three observational constraints, we increased the matter density. As we argued, this should have the effect of shifting the weak lensing distribution towards lower values of ϖ_0 , with the primary concern to determine whether $\varpi_0 = 0$ is allowed. Increasing the matter density also has the effect of moving the CMB distribution towards higher values, away from $\varpi_0 = 0$, and moves the ISW-galaxy cross-correlation towards more negative values, also away from $\varpi_0 = 0$. Using the WMAP3+SNGold ML model parameters, as shown in Figure 16, the overlap is improved. The tension between weak lensing and ISW is somewhat relaxed, with a joint likelihood that allows $\varpi_0 = 0$. Whether $\varpi_0 = 0$ is preferred remains to be demonstrated. A full, multi-dimensional parameter space analysis is planned for a subsequent paper.

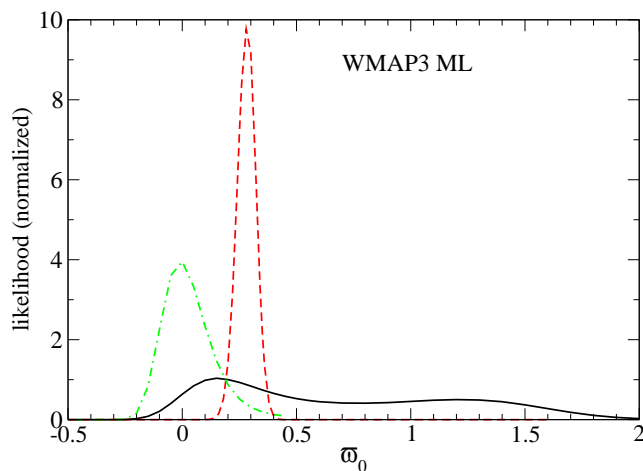


FIG. 15: The likelihood distributions for ϖ_0 , based on the CMB (solid curve), weak lensing (dashed), and ISW-galaxy cross correlation (dot-dashed) using the WMAP3 ML model parameters is shown.

IX. DISCUSSION

A PPF formalism for modified gravity has been proposed to describe possible departures from cosmological predictions under GR. The model consists of a background cosmology, a parameterized relationship between the gravitational potentials, and an implementation of new evolution equations in the absence of the perturbed Einstein's equations. For simplicity we have focused on the case in which the background cosmology evolves as a standard, Λ CDM universe. The gravitational slip is chosen to evolve in proportion to the dominance of an effective dark energy density over matter. The constant of proportionality introduces a new parameter, ϖ_0 . The

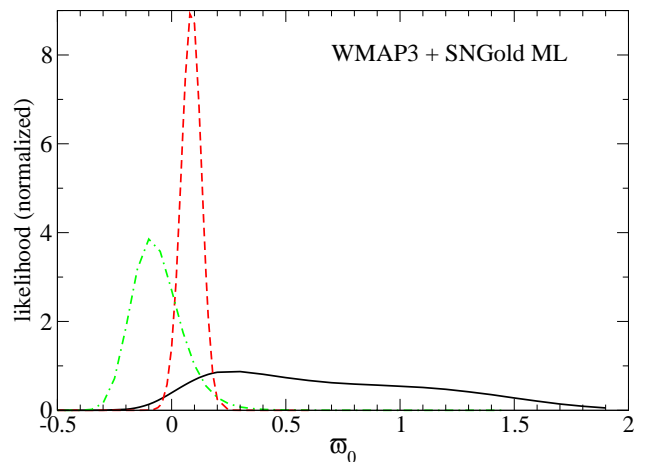


FIG. 16: The likelihood distributions for ϖ_0 , based on the CMB (solid curve), weak lensing (dashed), and ISW-galaxy cross correlation (dot-dashed) using the WMAP3+SNGold ML model parameters is shown.

new evolution equations are summarized by equations (14-16).

We have made a comparison between our proposed PPF model of modified gravitation and other models that have recently appeared in the literature. Our implementation satisfies the consistency relation proposed by Bertschinger [11]. Furthermore, the equivalence with the model of BZ has been demonstrated, after accounting for the correspondence between $\varpi(z)$ and $\gamma_{BZ}(a)$, using analytical calculations and numerical results.

We remark that many different parameterizations for the departure from GR on cosmological scales have been introduced in the literature. This variety may be useful, as no single model of non-Einstein gravitation stands out. However, it would also be useful if the data are compared within a single parameterization, similar to the post-Newtonian parameter γ_{PPN} that is used to measure the amount of spacetime curvature per unit mass in tests of gravitation in the solar system. In that regard, our parameter corresponds to $\varpi \approx 1 - \gamma_{PPN}$ in the limit of weak departures from GR. When ϖ is positive, then the gravitational potential determined by geodesic motion is greater than the potential inferred from the distribution of matter via the Poisson equation.

An alternative view of the gravitational slip is that it effectively introduces a new source for the perturbed off-diagonal space-space Einstein equation. If we infer the existence of some new density perturbations, defined so as to balance the perturbed time-time Einstein equation, then the new source takes the simple form $\frac{1}{3}\varpi \delta\rho_{tot}$.

We have corrected an error in CCM, and proceeded to examine the cosmological consequences of $\varpi_0 \neq 0$. We hope our study clarifies that: (a) there is a tension in current data that may be suggestive of PPF modifications of GR; (b) different parameterizations produce the same results at the end as long as certain consistency relations are satisfied; and (c) it would be useful to establish one

or two (and same) parameters from future data to finely test the departures from GR at cosmological scales.

APPENDIX A: EQUIVALENCE BETWEEN MODELS OF PPF GRAVITATIONAL SLIP

Bertschinger and Zukin [26] propose that ϕ evolves according to equation (19) after $z = 30$, with constant curvature perturbations, ζ . To show that their model is consistent with $\varpi\Lambda$ CDM, their evolution equation is recast as

$$\begin{aligned}\zeta &= \phi + \frac{\dot{\phi} + \mathcal{H}\psi}{\mathcal{H}(1 - \dot{\mathcal{H}})} \\ &= \eta + \frac{2}{3} \frac{\dot{\eta}}{\mathcal{H}(1 + w)}\end{aligned}\quad (\text{A1})$$

where the translation from conformal-Newtonian (longitudinal) gauge to synchronous gauge,

$$\phi = \eta - \mathcal{H}\alpha \quad (\text{A2})$$

$$\psi = \dot{\alpha} + \mathcal{H}\alpha, \quad (\text{A3})$$

is used in the second equality. Also, in a matter- and Λ -filled universe, $\mathcal{H}(1 - \dot{\mathcal{H}}/\mathcal{H}^2) = \frac{3}{2}\mathcal{H}(1 + w)$ where w is the background equation of state.

For consistency with the $\varpi\Lambda$ CDM model, the evolution of η , $\dot{\eta}$ according to equations (14-16) must agree that ζ as given in equation (A1) is a constant. Hence, assuming the zero- i perturbed Einstein equation (equation 21b of [10]) then

$$\begin{aligned}\zeta &= \eta + \left(\frac{2}{3}\right) \frac{4\pi G a^2 (\rho + p) \theta}{k^2 \mathcal{H}(1 + w)} \\ &= \eta + \frac{\mathcal{H}\theta}{k^2}\end{aligned}$$

where the background Friedmann equation is used to get the second equality. Taking a derivative with respect to conformal time,

$$\dot{\zeta} = \dot{\eta} + \frac{\dot{\mathcal{H}}\theta}{k^2} + \frac{\mathcal{H}\dot{\theta}}{k^2}. \quad (\text{A4})$$

Again using the zero- i Einstein equation, and the equation for $\dot{\theta}$ derived from stress-energy conservation (equation 29 of [10]),

$$\dot{\theta} = -\mathcal{H}(1 - 3w)\theta - \frac{\dot{w}}{1 + w}\theta + \frac{\delta p/\delta\rho}{1 + w}k^2\delta - k^2\sigma, \quad (\text{A5})$$

then the time derivative of the curvature perturbation is

$$\dot{\zeta} = \mathcal{H}\left(\frac{\delta p}{\delta\rho} \frac{\delta}{1 + w} - \sigma\right). \quad (\text{A6})$$

Since the dominant perturbations at late times ($z < 30$) are due to baryonic and dark matter that have negligible pressure and shear perturbations, then $\dot{\zeta} \approx 0$. Therefore, $\varpi\Lambda$ CDM is consistent with the evolution equation (A1) with constant ζ .

ACKNOWLEDGMENTS

It is a pleasure to thank Tommaso Giannantonio for help. SFD and RRC were supported in part by NSF CAREER AST-0349213. AC was supported by NSF CAREER AST-0645427. AC, SFD, and RRC thank the Theoretical Astrophysics Group at Caltech for hospitality while this research was conducted. AM research has been supported by ASI contract I/016/07/0 “COFIS”.

-
- [1] J. P. Uzan, *Gen. Rel. Grav.* **39**, 307 (2007) [arXiv:astro-ph/0605313].
 - [2] S. M. Carroll, A. De Felice, V. Duvvuri, D. A. Easson, M. Trodden and M. S. Turner, *Phys. Rev. D* **71**, 063513 (2005) [arXiv:astro-ph/0410031].
 - [3] S. Nojiri and S. D. Odintsov, *Int. J. Geom. Meth. Mod. Phys.* **4**, 115 (2007) [arXiv:hep-th/0601213].
 - [4] M. Ishak, A. Upadhye and D. N. Spergel, *Phys. Rev. D* **74**, 043513 (2006) [arXiv:astro-ph/0507184].
 - [5] S. Wang, L. Hui, M. May, and Z. Haiman, *Phys. Rev. D* **76**, 063503 (2007). [arXiv:0705.0165 [astro-ph]].
 - [6] D. Huterer and E. V. Linder, *Phys. Rev. D* **75**, 023519 (2007) [arXiv:astro-ph/0608681].
 - [7] E. V. Linder and R. N. Cahn, *Astropart. Phys.* **28**, 481 (2007) [arXiv:astro-ph/0701317].
 - [8] C. Di Porto and L. Amendola, arXiv:0707.2686 [astro-ph].
 - [9] S. Nesseris and L. Perivolaropoulos, arXiv:0710.1092 [astro-ph].
 - [10] C. P. Ma and E. Bertschinger, *Astrophys. J.* **455**, 7 (1995) [arXiv:astro-ph/9506072].
 - [11] E. Bertschinger, *Astrophys. J.* **648**, 797 (2006) [arXiv:astro-ph/0604485].
 - [12] C. Schmid, J. P. Uzan and A. Riazuelo, *Phys. Rev. D* **71**, 083512 (2005) [arXiv:astro-ph/0412120].
 - [13] V. Acquaviva, C. Baccigalupi and F. Perrotta, *Phys. Rev. D* **70**, 023515 (2004) [arXiv:astro-ph/0403654].
 - [14] P. Zhang, *Phys. Rev. D* **73**, 123504 (2006) [arXiv:astro-ph/0511218].
 - [15] C. Skordis, *Phys. Rev. D* **74**, 103513 (2006) [arXiv:astro-ph/0511591].
 - [16] G. R. Dvali, G. Gabadadze, and M. Porrati, *Phys. Lett. B* **485**, 208 (2000).
 - [17] A. Lue, *Phys. Rept.* **423**, 1 (2006) [arXiv:astro-ph/0510068].
 - [18] Y. S. Song, I. Sawicki and W. Hu, *Phys. Rev. D* **75**, 064003 (2007) [arXiv:astro-ph/0606286].
 - [19] M. V. Bebronne and P. G. Tinyakov, *Phys. Rev. D* **76**,

- 084011 (2007) [arXiv:0705.1301 [astro-ph]].
- [20] A. Lue, R. Scoccimarro and G. Starkman, Phys. Rev. D **69**, 044005 (2004) [arXiv:astro-ph/0307034].
- [21] P. Zhang, M. Liguori, R. Bean and S. Dodelson, arXiv:0704.1932 [astro-ph].
- [22] L. Amendola, M. Kunz and D. Sapone, arXiv:0704.2421 [astro-ph].
- [23] F. Schmidt, M. Liguori and S. Dodelson, Phys. Rev. D **76**, 083518 (2007) [arXiv:0706.1775 [astro-ph]].
- [24] M. A. Amin, R. V. Wagoner and R. D. Blandford, arXiv:0708.1793 [astro-ph].
- [25] B. Jain and P. Zhang, arXiv:0709.2375 [astro-ph].
- [26] E. Bertschinger and P. Zukin, arXiv:0801.2431 [astro-ph]. (BZ)
- [27] W. Hu and I. Sawicki, Phys. Rev. D **76**, 104043 (2007) [arXiv:0708.1190 [astro-ph]].
- [28] W. Hu, arXiv:0801.2433 [astro-ph].
- [29] R. Caldwell, A. Cooray and A. Melchiorri, Phys. Rev. D **76**, 023507 (2007) [arXiv:astro-ph/0703375]. (CCM)
- [30] U. Seljak and M. Zaldarriaga, Astrophys. J. **469**, 437 (1996).
- [31] <http://lambda.gsfc.nasa.gov>
- [32] C. Sealfon, L. Verde and R. Jimenez, Phys. Rev. D **71**, 083004 (2005) [arXiv:astro-ph/0404111].
- [33] O. Dore *et al.*, arXiv:0712.1599 [astro-ph].
- [34] D. N. Spergel *et al.* [WMAP Collaboration], Astrophys. J. Suppl. **170**, 377 (2007) [arXiv:astro-ph/0603449].
- [35] L. Guzzo *et al.*, Nature, **451**, 541 (2008).
- [36] M. Bartelmann and P. Schneider, Phys. Rept. **340**, 291 (2001) [arXiv:astro-ph/9912508].
- [37] R. D. Blandford, A. B. Saust, T. G. Brainerd, J. V. Villumsen, Mon. Not. Roy. Astron. Soc. **251**, 60 (1991)
- [38] N. Kaiser, Astrophys. J. **388**, 286 (1992).
- [39] J. Miralda-Escudé, Astrophys. J. **380**, 1 (1991).
- [40] A. Cooray, W. Hu and J. Miralda-Escudé, Astrophys. J. **535**, L9 (2000) [arXiv:astro-ph/0003205].
- [41] J. A. Peacock and S. J. Dodds, Mon. Not. Roy. Astron. Soc. **280**, L19 (1996) [arXiv:astro-ph/9603031].
- [42] S. M. Carroll, W. H. Press and E. L. Turner, Ann. Rev. Astron. Astrophys. **30**, 499 (1992).
- [43] L. Fu *et al.*, arXiv:0712.0884 [astro-ph].
- [44] A. Stebbins, arXiv:astro-ph/9609149.
- [45] J. Benjamin *et al.*, arXiv:astro-ph/0703570.
- [46] D. Munshi, P. Valageas, L. Van Waerbeke and A. Heavens, arXiv:astro-ph/0612667.
- [47] M. Jarvis, B. Jain, G. Bernstein and D. Dolney, Astrophys. J. **644**, 71 (2006) [arXiv:astro-ph/0502243].
- [48] H. Hoekstra *et al.*, Astrophys. J. **647**, 116 (2006) [arXiv:astro-ph/0511089].
- [49] R. G. Crittenden and N. Turok, Phys. Rev. Lett. **76**, 575 (1996) [arXiv:astro-ph/9510072].
- [50] A. Cooray, Phys. Rev. D **65**, 103510 (2002) [arXiv:astro-ph/0112408].
- [51] N. Afshordi, Phys. Rev. D **70**, 083536 (2004) [arXiv:astro-ph/0401166].
- [52] P. S. Corasaniti, T. Giannantonio and A. Melchiorri, Phys. Rev. D **71**, 123521 (2005).
- [53] J. Garriga, L. Pogosian and T. Vachaspati, Phys. Rev. D **69**, 063511 (2004).
- [54] L. Pogosian, JCAP **0504**, 015 (2005).
- [55] P. Fosalba, E. Gaztanaga and F. Castander, Astrophys. J. **597**, L89 (2003).
- [56] S. Boughn and R. Crittenden, Nature **427**, 45 (2004).
- [57] R. Scranton *et al.* [SDSS Collaboration], arXiv:astro-ph/0307335.
- [58] M. R.olta *et al.* [WMAP Collaboration], Astrophys. J. **608**, 10 (2004).
- [59] N. Afshordi, Y. S. Loh and M. A. Strauss, Phys. Rev. D **69**, 083524 (2004).
- [60] T. Giannantonio *et al.*, Phys. Rev. D **74**, 063520 (2006).
- [61] E. Gaztanaga, M. Manera and T. Multamaki, Mon. Not. Roy. Astron. Soc. **365**, 171 (2006) [arXiv:astro-ph/0407022].
- [62] A. Cabre, E. Gaztanaga, M. Manera, P. Fosalba and F. Castander, Mon. Not. Roy. Astron. Soc. Lett. **372**, L23 (2006) [arXiv:astro-ph/0603690].